

Thermodynamics of thallium alkanoates

VI. Thallium(I) *n*-heptanoate revisited^a

A.K. LABBAN, F. L. LÓPEZ DE LA FUENTE,^b J. A. R. CHEDA,^b
EDGAR F. WESTRUM, JR., and F. FERNÁNDEZ-MARTÍN^c

*Department of Chemistry, University of Michigan,
Ann Arbor, MI 48109, U.S.A.*

(Received 2 January 1989)

The heat capacity of thallium(I) *n*-heptanoate has been remeasured on a new sample on which the preparative procedures were modified to eliminate the 1–1 (salt + acid) complex (soap) in a previously studied sample. The sub-ambient heat capacity of a new highly pure thallium(I) *n*-heptanoate is characterized by one set of transitions between 262 and 272 K and another transition at 301 K. The lowest transition temperature at 262.1 K has a maximum of $C_{p,m} \approx 559R$. Next, a bifurcated pair (at 268.6 and 271.4 K) have $C_{p,m} \approx 300R$, and the highest transition (at 301.0 K) has a maximum $C_{p,m} \approx 1697R$. The corresponding values of $\Delta_{\text{trs}}S_m^\circ$ for the two sets are about 2.24R and 1.10R. At 298.15 K the values of $\Delta_0^T S_m^\circ$, $\Delta_0^T H_m^\circ$, and $\Phi_m^\circ(T)$ are 39.79R, 5979R·K, and 19.74R. Smoothed thermodynamic functions at selected temperatures are tabulated through melting.

1. Introduction

In the course of measurement of the series of thallium alkanoates,^(1–4) it was noted subsequent to submission for publication of the results for the thallium(I) *n*-heptanoate⁽²⁾ that of the five transitions observed in the 260 to 310 K region, one of the larger ones at ≈ 296 K was indeed extraneous. Subsequent studies on the phase behavior of the (salt + acid) system revealed⁽⁵⁾ that a unimolecular (salt + acid) complex is formed and that several per cent of this contaminated the previous sample. The presence of such 1–1 acid soaps has been demonstrated in alkali laurates, stearates, and oleates by various techniques^(6–8) and complexes with higher (salt + acid) ratios have also been claimed.

Subsequent analysis based on $\Delta_{\text{trs}}H_m$ against x_{salt} values from the corresponding phase diagram,⁽⁵⁾ showed the previous sample to contain about (9 ± 1) moles per cent of acid⁽²⁾ and to differ from data of Fernández-Martín *et al.*,⁽⁹⁾ who did not find the

^a The first paper in this series is reference 1.

^b Address: Departamento de Química Física, Facultad de Ciencias Químicas, Universidad Complutense, 28040 Madrid, Spain.

^c Address: Instituto del Frío, CSIC, 28040 Madrid, Spain.

transition at 296.2 K. This paper reports measurements on a new carefully purified sample judged to be 99.7 moles per cent pure and free of the complex. The former III-to-II transition is not present. Consequently, the numbering of phases >III originally designated by Ngeyi *et al.*⁽²⁾ must here be reduced by unity. That is, his phase VI becomes V, *etc.*, in the present work. Further studies on the thermophysics of the acid and the 1-1 complex are underway. Previous studies on related systems have been summarized.⁽¹⁰⁾

2. Experimental

The sample of Tl7C used in this study—designated 86-Tl7C hereafter—was prepared by reacting heptanoic acid (Fluka, puriss grade, >99 moles per cent, tested by g.c. at the origin) dissolved in anhydrous methanol with a slight excess (≈ 5 per cent) of the stoichiometric amount of Tl_2CO_3 , suspended in the same solvent. After refluxing under stirring for several hours and separating the excess of Tl_2CO_3 by filtration, the clear solution was concentrated until incipient crystallization of the salt occurred and precipitation was completed by adding dry ethyl ether. After filtration, the recovered powdered crystals were purified by repeated recrystallizations from absolute ethanol. The salt was finally vacuum-dried at room temperature to constant mass. I.r. spectroscopic determinations showed no traces of water or free acid. Moreover, several d.s.c. purity determinations by a fractional-fusion technique yielded a mean value of (99.7 ± 0.1) moles per cent of liquid-soluble solid-insoluble purity. The difference between the method described and that used to synthesize the sample first studied⁽²⁾ (84-Tl7C, hereafter) is small. Then, we had followed the method described elsewhere⁽¹¹⁾ and the advice of Duruz *et al.*⁽¹²⁾ According to them, the decomposition rates for the homologous series of sodium alkanoates are quite high unless a small excess of organic acid is introduced in the reaction medium; they explain that the addition of an excess of acid represses the action of the free hydroxyl ion, considered as the main cause of instability of such salts. Perhaps this assertion is valid only for syntheses in which the water is the solvent—as in the case of Na alkanoates—but even in the case of other compounds prepared in anhydrous methanol, as Cs alkanoates,⁽¹³⁾ a slight excess of acid had been also used. Hence, we had also used this method for preparing the 84-Tl7C sample which became contaminated by heptanoic acid. This, however, could not be demonstrated until careful comparisons were made with other samples of thallium(I) heptanoate, prepared under different conditions, resulting ultimately in a study of the (Tl7C + HC7) phase diagram.⁽⁵⁾

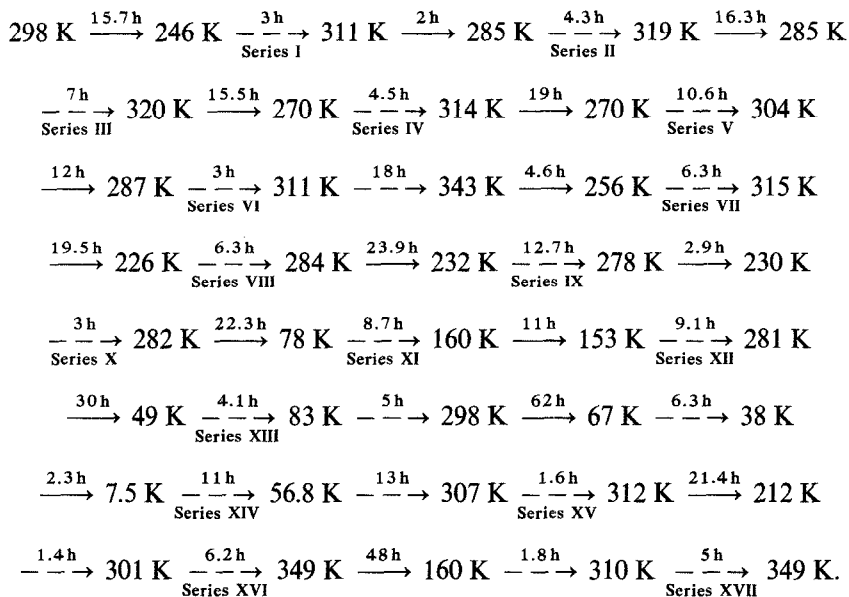
CALORIMETRIC PROCEDURE

Measurements were made from 8 to 350 K in the adiabatic Mark-X calorimetric cryostat previously described^(2, 14, 15) by an automated intermittent-heating quasi-adiabatic technique.⁽¹⁵⁾

The sample loaded into the gold-plated copper calorimeter designated W-AB had a mass of 36.419 g corresponding to a reciprocal amount of substance of 9.1587 mol^{-1} with molar mass of $333.55 \text{ g} \cdot \text{mol}^{-1}$ (on the basis of the 1978 IUPAC

atomic masses). The buoyancy corrections were calculated assuming a density of $2.85 \text{ g} \cdot \text{cm}^{-3}$. Following evacuation, 21.0 kPa of purified helium was added to the calorimeter to promote thermal equilibrium.

The thermal history of the thallium(I) *n*-heptanoate is shown by the linear array; solid arrows indicate cooling and dashed arrows indicate results-acquisition (heating) ranges for various series.



Other procedural matters are comparable to those described in the previous measurements.⁽²⁾

3. Results and discussion

The experimental heat capacities are given in table 1 and plotted for the transition in figure 1. These results are listed in chronological order. Within a series, the temperature interval of each measurement may usually be inferred from the mean temperatures of adjacent determinations.

The heat capacities were fitted to a series of orthogonal polynomials in regions of normal heat capacity. In the transition region, other methods were used to obtain the total and excess enthalpies and the entropies.

Four presumably first-order transitions were observed in the heat-capacity curve defined by our measurements. The detail of heat-capacity peaks are shown in figure 2. The reproducibility of the heat-capacity curve in our measurements is shown in table 2 for several determinations through this transition region.

Integration of the polynomials and the transitions yielded the thermodynamic

TABLE 1. Experimental values of heat capacity of thallium(I) *n*-heptanoate ($R = 8.3144 \text{ J} \cdot \text{K}^{-1} \cdot \text{mol}^{-1}$)

<i>T</i> /K	$C_{p,m}/R$	<i>T</i> /K	$C_{p,m}/R$	<i>T</i> /K	$C_{p,m}/R$	<i>T</i> /K	$C_{p,m}/R$	<i>T</i> /K	$C_{p,m}/R$
Series I		296.50	40.31	240.85	26.50	126.84	16.61	17.56	2.113
		297.37	41.51	246.56	27.46	131.92	17.00	18.67	2.341
251.26	28.38	298.22	43.62	252.12	28.65	137.02	17.36	19.78	2.572
257.26	29.96	299.22	44.82	255.38	28.89	142.12	17.67	20.91	2.806
303.61	67.98	300.56	78.42	256.39	29.76	147.23	18.00	22.05	3.044
307.85	38.59	300.92	1003	257.40	29.90	152.34	18.35	23.93	3.440
310.46	38.73	300.955	1620	258.40	30.59	157.45	18.70	25.87	3.859
		300.964	1697	259.40	30.30			27.17	4.134
Series II		300.997	843	260.38	41.47	Series XII		28.52	4.415
286.40	34.76	301.34	69.7	261.36	36.42	155.86	18.56	29.86	4.704
288.23	35.41	302.21	41.93	261.96	186.9	161.58	18.95	31.21	4.982
290.69	36.31	303.27	40.85	262.11	558	167.70	19.35	32.61	5.286
$\Delta_{rs}H_m$	Detn. A	304.36	39.77	262.19	480	173.84	19.74	34.07	5.563
305.96	38.88			262.28	358	179.97	20.22	35.60	5.868
309.05	38.56	Series VI		262.38	267.4	186.09	20.67	37.03	6.099
312.18	38.28	288.58	35.46	263.15	40.70	192.23	21.13	38.87 ^a	6.664
315.31	38.36	290.93	36.02	264.55	30.72	198.36	21.66	41.11	6.977
318.43	38.10	$\Delta_{rs}H_m$	Detn. D	266.08	31.30	205.37	22.24	43.35	7.350
				267.44	43.57	211.51	22.86	45.57	7.789
Series III		Series VII		268.30	134.7	217.63	23.48	47.95	8.181
284.17	34.32	295.15	41.52	268.64	307.7	223.76	24.17	50.48	8.603
285.96	34.73	265.45	39.99	269.32	48.86	229.88	24.79	53.01	9.036
288.34	35.17	269.98	115.9	270.25	36.15	234.22	25.53		
290.68	36.21	276.85 ^a	15.37	270.90	40.18	236.53	25.97	Series XV	
$\Delta_{rs}H_m$	Detn. B	283.60 ^a	109.2	271.27	231.2	$\Delta_{rs}H_m$	Detn. G	310.02 ^a	37.84
305.64	38.88	285.94	34.71	271.40	285.7	276.87	33.09	Series XVI	
306.90	38.72	287.68	35.41	271.83	93.06	279.86	33.60	303.11	41.04
308.99	38.39	289.44	35.82	272.81	42.92			307.81	38.62
312.12	38.17	$\Delta_{rs}H_m$	Detn. E	274.23	33.87	Series XIII		313.15 ^b	38.25
315.24	38.24	305.55	38.98	275.78	33.04	50.49	8.579	318.32 ^a	37.83
318.36	38.19	309.50 ^a	44.09	277.33	33.35	53.16	9.031	323.47 ^a	38.30
		313.67 ^a	33.36	Series X		56.08	9.474	328.67	37.46
Series IV		Series VIII		233.36	25.30	59.25	9.947	333.84	37.47
284.19	34.39	299.39	24.85	237.15	25.83	62.66	10.495	339.10	36.97
285.67	34.74	235.36	25.66	239.20	26.00	66.09	10.866	343.82	36.52
287.42	35.18	241.19	26.60	$\Delta_{rs}H_m$	Detn. F	69.77	11.378	347.46	36.42
289.17	36.04	246.89	27.55	280.18	33.61	73.71	11.847		
290.92	36.43	252.45	28.70	Series XI		77.66	12.312	Series XVII	
$\Delta_{rs}H_m$	Detn. C	257.85	30.27	80.97	12.72	Series XIV		314.19 ^a	35.83
307.82	38.43	261.32	136.13	85.01	13.17	7.54 ^a	0.374	320.35 ^b	37.99
312.87	38.19	263.79	58.39	89.00	13.60	8.73	0.482	322.95 ^a	15.54
Series V		267.02	63.30	93.02	13.92	9.83	0.649	325.70 ^a	39.28
276.93	33.18	269.97	73.44	97.06	14.23	10.65	0.793	330.94	37.59
286.15	34.76	272.80	63.19	101.59	14.63	11.51	0.948	336.27	37.24
289.99	35.84	276.86	33.44	106.63	14.98	12.39 ^b	1.106	341.63	36.97
291.36	37.13	281.81	34.02	111.66	15.43	13.30	1.267	345.66 ^a	36.10
292.74	37.48	Series IX		116.70	15.86	14.30 ^b	1.457	348.34	36.25
294.08	38.15	235.01	25.63	121.76	16.27	15.37	1.677		
295.40	39.40					16.45	1.889		

^a Not used in final fit. ^b Corrected and used in final fit.

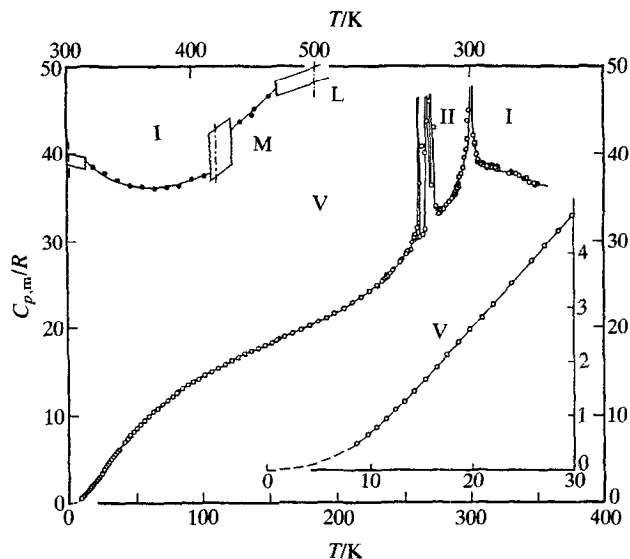


FIGURE 1. Experimental molar heat capacities at constant pressure plotted against temperature for thallium(I) *n*-heptanoate $C_6H_{13}CO_2Tl$. \circ , This work; \bullet , from reference 2.

functions. Tabulation of the smoothed values of $C_{p,m}/R$ and derived functions is given for selected temperatures in table 3.

In table 4, a summary of the observed transition temperatures and thermodynamic-property increments and literature values are given for comparison. (The revised numbering of the phases, and designations of the transitions, in table 4 is that adopted in this work.) It can be observed that the sum of the increments of thermal functions of the transitions IV-to-III and III-to-II are almost identical for both adiabatic and d.s.c. techniques, but the individual values of each transition are interchanged.

D.s.c. cooling and heating thermograms ($0.17 \text{ K} \cdot \text{s}^{-1}$) given in figure 3 show a thermal hysteresis. The continuous line of the cooling curve consists of three peaks while the corresponding heating curve shows four peaks, instead. The area of the first and the last exothermic peaks correspond to those of the last II-to-I (at 301.9 K) and the first V-to-IV (at 262.3 K) endothermic peaks, respectively. The second exothermic peak is converted into a bifurcated pair of endothermic peaks (IV-to-III at 267.9 K, and III-to-II at 272.4 K) with a small shoulder (at 271.1 K), but the areas involved in both cases are approximately the same. On the other hand, another kind of metastability is observed when the cooling step is stopped at about 250 K; once, a second exothermic peak appeared in the cooling thermogram. The heating thermogram is then recorded (dotted curves). Here, the metastable second exothermic peak is converted into two symmetric endothermic peaks (IV'-to-III' at 269.3 K, and III'-to-II at 271.8 K), with the total area remaining approximately the same as previously. In addition, the first endothermic peak at 262.3 K does not

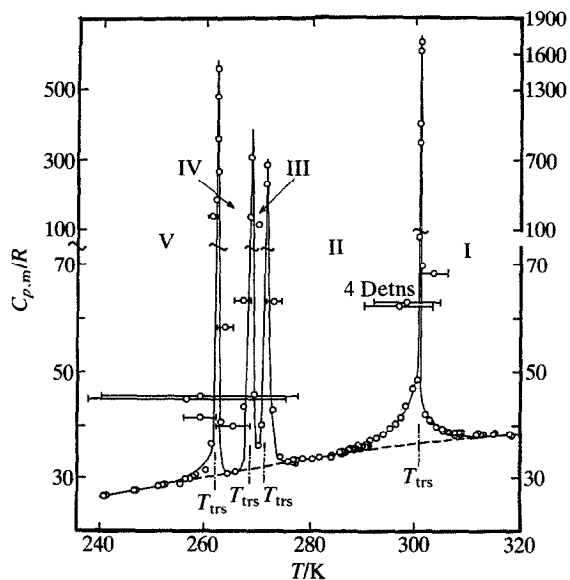


FIGURE 2. Experimental molar heat capacities at constant pressure plotted against temperature through the transition region from 240 to 320 K for thallium(I) *n*-heptanoate $C_6H_{13}CO_2Tl$.

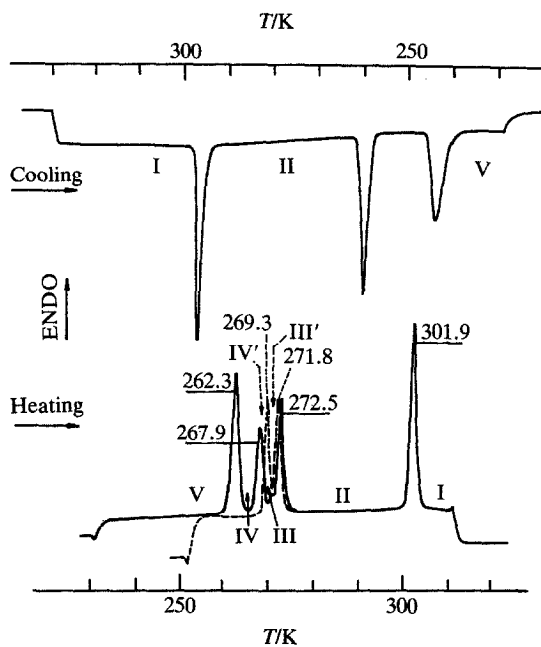


FIGURE 3. D.s.c. cooling and heating thermograms for thallium(I) *n*-heptanoate.

TABLE 2. Summary of transition thermophysical quantities for thallium(I) *n*-heptanoate ($R = 8.3144 \text{ J} \cdot \text{K}^{-1} \cdot \text{mol}^{-1}$)

Series	No. of detns	T_1/K	T_2/K	$\Delta_{T_2}^{T_1} H_m^\circ/(R \cdot \text{K})$	$\Delta_{235\text{K}}^{275\text{K}} H_m^\circ/(R \cdot \text{K})$	$\Delta_{235\text{K}}^{275\text{K}} S_m^\circ/R$
Transition set combining transitions V-to-IV, IV-to-III, and III-to-II						
VIII	9	238.3	274.4	1651.3	1758. ₀	
X	2 + Detn. F	236.12	277.69	1818.0	1757. ₂	
XII	1 + Detn. G	235.499	275.37	1756.23	1756. ₇	
Graphical integration:					1757. ₃ ^a	6.793 ± 0.003
Mean:					1757. ₃ ± 0.7	
Lattice contribution:					1163. ₉ ± 1.0	4.550 ± 0.004
$\Delta_{\text{trs}} H_m^\circ(\text{V-to-IV-to-III-to-II})/(R \cdot \text{K}) =$					593. ₄ ± 1	
$\Delta_{\text{trs}} S_m^\circ(\text{V-to-IV-to-III-to-II})/R =$						2.243 ± 0.004
$\Delta_{\text{V}}^{\text{IV}} H_m^\circ/(R \cdot \text{K}) = 257.2 \pm 1$					$\Delta_{\text{V}}^{\text{IV}} S_m^\circ/R = 0.995 \pm 0.004$	
$\Delta_{\text{IV}}^{\text{III}} H_m^\circ/(R \cdot \text{K}) = 189.7 \pm 1$					$\Delta_{\text{IV}}^{\text{III}} S_m^\circ/R = 0.707 \pm 0.004$	
$\Delta_{\text{III}}^{\text{II}} H_m^\circ/(R \cdot \text{K}) = 146.s \pm 1$					$\Delta_{\text{III}}^{\text{II}} S_m^\circ/R = 0.541 \pm 0.003$	
Transition II to I					$\Delta_{290\text{K}}^{305\text{K}} H_m^\circ/(R \cdot \text{K})$	$\Delta_{290\text{K}}^{305\text{K}} S_m^\circ/R$
II	1 + Detn. A	289.46	304.97	909.0	890.6	
III	1 + Detn. B	289.51	304.89	905.1	892.8	
IV	1 + Detn. C	290.04	304.85	884.0	891.2	
Graphical integration:					891.2 ^a	
Mean:					891.1 ± 0.6	2.981 ± 0.002
Lattice contribution:					529.2 ± 1	1.820 ± 0.004
$\Delta_{\text{II}}^{\text{I}} H_m^\circ/(R \cdot \text{K}) =$					361.9 ± 1	
$\Delta_{\text{II}}^{\text{I}} S_m^\circ/R =$						1.194 ± 0.004

^a Not included in the mean value.

appear at all, while the new solid metastable form IV' presents a higher heat capacity than that of the solid stable form V. On tempering the sample at 250 K, the thus-cooled sample evolves slowly towards the stable situation.

Compared with the heat-capacity values observed in this study, those of Ngeyi *et al.*⁽²⁾ were 2.7 per cent higher below 50 K, about 2.5 per cent higher above 50 K, and more than 5 per cent higher above 300 K. At subambient temperatures, the values of the total enthalpy and entropy for the same set of transitions are about 9 per cent lower than the values observed in this study. These differences, noted in table 5, are due not only to the absence of acid—and hence of (acid + salt) complex—in the present sample, but also the different evaluation of interpolated lattice heat capacities in transition regions. Taking into account arbitrarily different assignments of lattice heat capacity between the Ngeyi *et al.*⁽²⁾ paper and the present work and the inability to resolve exactly the overlapping premonitory and post-transitional effects in the trifurcated lower set of transitions, a convincing comparison can be made only by summing the lower set of transitions. When this is done (see table 5) the present measurements are seen to give enthalpy increments about 9 per cent higher, *i.e.* they are proportional to the amount of salt present. The transition

TABLE 3. Thermodynamic properties of thallium(I) *n*-heptanoate ($R = 8.3144 \text{ J} \cdot \text{K}^{-1} \cdot \text{mol}^{-1}$)

$\frac{T}{\text{K}}$	$\frac{C_{p,m}}{R}$	$\frac{\Delta_0^T S_m^\circ}{R}$	$\frac{\Delta_0^T H_m^\circ}{R \cdot \text{K}}$	$\frac{\Phi_m^\circ(T)}{R}$	$\frac{T}{\text{K}}$	$\frac{C_{p,m}}{R}$	$\frac{\Delta_0^T S_m^\circ}{R}$	$\frac{\Delta_0^T H_m^\circ}{R \cdot \text{K}}$	$\frac{\Phi_m^\circ(T)}{R}$
Phase V					Phase III				
0	0	0	0	0	268.64 ^a	(308)	(35.71)	(4827)	(17.73)
5	0.164	(0.055)	(0.205)	(0.014)		[31.62]	(34.00)	[4380]	[17.69]
10	0.681	0.274	1.941	0.080	270 ^b	35.00	(35.86)	(4870)	(17.82)
15	1.600	0.720	7.594	0.214		[31.88]	(34.16)	[4423]	[17.78]
20	2.614	1.318	18.096	0.413	271.40 ^a	(285)	(36.03)	(4915)	(17.92)
						[32.11]	[34.33]	[4468]	[17.87]
25	3.678	2.015	33.818	0.662					
30	4.728	2.779	54.85	0.950					
					Phase II				
40	6.733	4.416	112.24	1.610	271.40 ^a	(285)	(36.57)	(5061)	(17.92)
50	8.526	6.117	188.80	2.341		[32.11]	[34.33]	[4468]	[17.87]
60	10.069	7.811	281.93	3.112	275	(32.80)	(36.99)	(5178)	(18.16)
						[32.79]	[34.75]	[4585]	[18.08]
70	11.423	9.467	389.55	3.902					
80	12.599	11.071	509.8	4.698	280	33.64	(37.59)	(5344)	(18.50)
90	13.624	12.615	641.0	5.493		[33.64]	[35.35]	[4751]	[18.38]
100	14.530	14.098	781.9	6.280					
120	16.10	16.89	1088.6	7.819	290	35.13	(38.80)	(5688)	(19.19)
						(35.13)	[36.56]	[5095]	[18.99]
140	17.51	19.48	1424.8	9.302					
160	18.86	21.91	1788.6	10.727	298.15	42.6	39.79	5979	19.74
180	20.24	24.21	2179.5	12.098	300.96 ^a	(1700)	(40.13)	(6081)	(19.92)
200	21.74	26.41	2598.9	13.420		[36.52]	[37.89]	[5488]	[19.65]
220	23.68	28.57	3052.1	14.699					
					Phase I				
240	26.41	30.74	3551.4	15.95					
260	29.98	32.99	4114.2	17.17	300.96 ^a	(1700)	(41.29)	(6431)	(19.92)
262.11 ^a	(558)	(33.23)	(4178)	(17.29)		[36.52]	[37.89]	[5488]	[19.65]
	[30.41]	[33.23]	[4178]	[17.29]	310	(37.40)	(42.38)	(6765)	(20.56)
						[37.40]	[38.98]	[5822]	[20.20]
					Phase IV				
262.11 ^a	(558)	(34.22)	(4435)	(17.29)	320	38.10	43.59	7144	21.26
	[30.41]	[33.23]	[4178]	[17.29]	340	36.98	45.86	7896	22.64
265 ^b	30.96	(34.56)	(4523)	(17.49)	350	36.22	(46.92)	(8261)	(23.32)
	[30.96]	[33.57]	[4266]	[17.47]					
268.64 ^a	(308)	(34.99)	(4637)	(17.73)					
	[31.62]	[34.00]	[4380]	[17.69]					

^a Values in parentheses represent thermodynamic functions for the experimental heat-capacity values on the assumption that they are truly isothermal at T_{trs} . Those in brackets represent the selected lattice (*i.e.* non-translational) heat capacity.

^b Quantities between close or bifurcated transitions when taken as on the lattice curve (see assumption in *a*) are also shown in parentheses. Values neither in parentheses or in brackets are thus (real) observed values at the selected temperatures.

previously observed near 296 K is not present and is presumed to be related to the presence of heptanoic acid on the phase behavior of the binary system—a point requiring further experimentation (which is presently underway). It is clearly not a transition in heptanoic acid as shown by our unpublished work, but is a major transition in the 1–1 (acid + salt) complex (soap) phase system.

TABLE 4. Summary of transition properties of thallium(I) *n*-heptanoate ($R = 8.3144 \text{ J} \cdot \text{K}^{-1} \cdot \text{mol}^{-1}$)

Transition	T_{trs}/K	$\Delta_{\text{trs}}H_{\text{m}}^{\circ}/(R \cdot \text{K})$	$\Delta_{\text{trs}}S_{\text{m}}^{\circ}/R$	Reference
IV'-to-III'	269.3	170	0.63	this work (d.s.c.)
III'-to-II	271.8	170	0.62	this work (d.s.c.)
V-to-IV	262.11	257.2	0.995	this work (a.c.)
	262.3	251	0.96	this work (d.s.c.)
IV-to-III	268.64	189.7	0.707	this work (a.c.)
	267.9	146	0.54	this work (d.s.c.)
III-to-II	271.4	146.5	0.541	this work (a.c.)
	272.4	191	0.70	this work (d.s.c.)
II-to-I	300.96	361.9	1.104	this work (a.c.)
	301.9	319	1.06	9
I-to-Mesophase	420.7	758	1.80	9
Mesophase-to-Isotropic liquid	502.0	397	0.79	9

TABLE 5. Comparison of cryogenic calorimetric transitions for thallium(I) *n*-heptanoate

Transition designation	T_{trs}/K		$\Delta_{\text{trs}}H_{\text{m}}^{\circ}/(R \cdot \text{K})$	
	This research	Ngeyi <i>et al.</i> ⁽²⁾	This research ^a	Ngeyi <i>et al.</i> ⁽²⁾
V-to-IV	262.1 ± 0.07	262.8 ± 0.08	593.4	544
IV-to-III	268.2 ± 0.1	267.8 ± 0.1		
III-to-II	271.4 ± 0.08	271.7 ± 0.3		
T_{trs}^b	Not present	296 ± 0.8	—	—
II-to-I	300.9 ± 0.06 ^d	300.9 ± 0.06	361.9	358

^a After adjustment of Ngeyi *et al.*⁽²⁾ lattice contribution to correspond to those of the present research.

^b T_{trs}^b refers to the transition seen by Ngeyi *et al.*⁽²⁾ near 296 K and not apparent in the present diagram.

^c By d.s.c., this research.

^d D.s.c. values of 301.9 and 299 K were determined by Fernández-Martín *et al.*⁽⁹⁾ and by Meisel *et al.*⁽¹¹⁾ respectively.

Although the post-transitional heat capacity is significantly different on the II-to-I transition and the estimation of its magnitude suffers from the same difficulties as the lower set, the $\Delta_{\text{trs}}H_{\text{m}}$ seems to be comparable in both sets of measurements.

The apparent differences in peak temperatures of the two sets of transitions is probably an indication of experimental resolution caused by the finite size of the temperature increments of the mapping runs rather than real differences occasioned by purity.

REFERENCES

- Boerio-Goates, J.; López de la Fuente, F. L.; Cheda, J. A. R.; Westrum, E. F., Jr. *J. Chem. Thermodynamics* **1985**, *17*, 401.
- Ngeyi, S. P.; López de la Fuente, F. L.; Cheda, J. A. R.; Fernández-Martín, F.; Westrum, E. F., Jr. *J. Chem. Thermodynamics* **1985**, *17*, 409.
- Ngeyi, S. P.; Westrum, E. F., Jr.; López de la Fuente, F. L.; Cheda, J. A. R.; Fernández-Martín, F. *J. Chem. Thermodynamics* **1987**, *19*, 327.

4. López de la Fuente, F. L.; Cheda, J. A. R.; Westrum, E. F., Jr.; Fernández-Martín, F. *J. Chem. Thermodynamics* **1987**, 19, 1261.
5. Fernández-Martín, F.; López de la Fuente, F. L.; Cheda, J. A. R.; Westrum, E. F., Jr. *XXI Bienal Real Sociedad Esp. Quim.* (1986).
6. Brouwer, H. W.; Spier, H. L. *Thermal Analysis*. Proceedings of the Third ICTA at Davos, Switzerland (1971). **1972**, Vol. 3, p. 131.
7. McBain, J. W.; Stewart, A. *J. Chem. Soc.* **1933**, 924.
8. McBain, J. W.; Stewart, A. *J. Chem. Soc.* **1927**, 1392.
9. Fernández-Martín, F.; López de la Fuente, F. L.; Cheda, J. A. R. *Thermochimica Acta* **1983**, 73, 109.
10. Franzosini, P.; Sanesi, M. *Thermodynamics and Transport Properties of Organic Salts*. Pergamon: London. **1980**.
11. Meisel, T.; Seybold, K.; Halmos, Z.; Roth, J.; Melykuti, Cs. *J. Therm. Anal.* **1976**, 10, 419.
12. Duruz, J. J.; Michels, M. J.; Ubbelohde, A. R. *Proc. Roy. Soc. Lond. A* **1971**, 322, 781.
13. Sanesi, M.; Franzosini, P. *Z. Naturforsch.* **1984**, 399, 362.
14. Westrum, E. F., Jr.; McCullough, J. P. *Experimental Thermodynamics*. Scott, D. W.; McCullough, J. P.: editors. Butterworths: New York. **1968**, p. 745.
15. Westrum, E. F., Jr. *Proceedings NATO Advanced Study Institute on Thermochemistry at Viana do Castelo, Portugal*. Ribeiro da Silva, M. A. V.: editor. Reidel: New York. **1984**, p. 745.